Supplementary Information of

Long-term evolution and effects of primary brown carbon aerosols in China

Guochao Chen[1], Yiheng Wang[1], Qi Ying[2], Xiaofei Wang[1,3], Hongliang Zhang[1,4,5,*]

[1]Department of Environmental Science and Engineering, Fudan University, Shanghai, 200438, China
[2]Division of Environment and Sustainability, Hong Kong University of Science and Technology, Hong Kong SAR, China
[3]Shanghai Institute of Pollution Control and Ecological Security, Shanghai 200092, China
[4]IRDR ICoE on Risk Interconnectivity and Governance on Weather/Climate Extremes Impact and Public Health, Fudan University, Shanghai 200438, China
[5]School of Environment and Architecture, University of Shanghai for Science and Technology, Shanghai, 200093, China

**Correspondence to*: Hongliang Zhang (zhanghl@usst.edu.cn)

Supplementary Tables and Figures

Table S1. Model performance on $PM_{2.5}$ and MDA8 O_3 in 2015 and 2020. (MFE is mean fractional error; MNB is mean normalized bias; MNE is mean normalized error). The performance criteria are suggested by EPA [1].

$PM_{2.5}$ ($\mu g\ m^{-3}$)	2015	2015.01	2015.02	2015.03	2015.04	2015.05	2015.06	2015.07	2015.08	2015.09	2015.10	2015.11	2015.12	Criteria
OBS	52.82	84.61	70.18	53.84	48.09	44.31	37.22	37.49	36.16	36.76	51.97	57.86	78.06	
PRE	56.98	71.12	69.24	61.69	55.77	42.40	36.91	40.67	47.39	51.07	62.31	68.30	77.68	
MNB	0.52	0.29	0.49	0.63	0.52	0.26	0.35	0.39	0.61	0.79	0.61	0.71	0.55	
MNE	1.04	0.92	1.02	1.08	1.00	0.87	0.96	0.93	1.07	1.24	1.09	1.19	1.08	
MFB	-0.06	-0.22	-0.09	0.02	-0.02	-0.21	-0.19	-0.11	0.01	0.07	-0.01	0.01	-0.07	$\leq \pm 0.6$
MFE	0.74	**0.76**	0.74	0.73	0.72	0.73	0.75	0.70	0.72	0.75	0.73	**0.77**	**0.76**	≤ 0.75
RMSE	63.81	83.57	73.27	58.77	57.70	48.47	43.81	43.37	47.40	51.43	63.07	81.75	91.49	
$PM_{2.5}$ ($\mu g\ m^{-3}$)	2016	2016.01	2016.02	2016.03	2016.04	2016.05	2016.06	2016.07	2016.08	2016.09	2016.10	2016.11	2016.12	Criteria
OBS	47.69	65.15	58.23	59.34	43.41	39.51	32.01	31.15	29.76	38.32	38.72	60.45	80.02	
PRE	50.21	61.50	61.11	59.89	49.66	38.25	35.33	33.50	40.01	52.79	43.61	61.22	67.65	
MNB	0.48	0.37	0.53	0.40	0.55	0.33	0.42	0.36	0.65	0.70	0.59	0.54	0.26	
MNE	1.02	0.94	1.03	0.93	1.08	0.94	0.98	0.93	1.10	1.15	1.13	1.12	0.88	
MFB	-0.09	-0.14	-0.03	-0.10	-0.06	-0.20	-0.13	-0.15	0.03	0.04	-0.07	-0.11	-0.23	$\leq \pm 0.6$
MFE	0.75	0.74	0.73	0.72	**0.76**	**0.77**	0.74	0.72	0.72	0.73	**0.77**	**0.81**	0.74	≤ 0.75
RMSE	58.71	70.44	67.80	70.82	53.46	52.77	38.90	36.53	41.67	53.34	48.51	74.29	78.45	
$PM_{2.5}$ ($\mu g\ m^{-3}$)	2017	2017.01	2017.02	2017.03	2017.04	2017.05	2017.06	2017.07	2017.08	2017.09	2017.10	2017.11	2017.12	Criteria
OBS	45.90	75.89	64.43	50.29	42.07	39.89	31.35	29.60	26.50	32.53	41.13	53.04	65.83	
PRE	47.87	55.86	64.82	52.50	47.50	39.22	39.60	34.00	36.57	44.60	52.01	50.62	57.54	
MNB	0.49	0.20	0.50	0.43	0.49	0.37	0.56	0.40	0.70	0.79	0.77	0.39	0.20	
MNE	1.02	0.87	1.02	0.93	1.02	0.94	1.06	0.91	1.17	1.25	1.23	1.05	0.84	

MFB	-0.09	-0.28	-0.07	-0.07	-0.07	-0.15	-0.04	-0.09	0.02	0.05	0.06	-0.21	-0.25	≤ ±0.6
MFE	0.74	**0.77**	0.74	0.70	0.75	0.75	0.72	0.68	0.74	0.74	**0.76**	**0.82**	0.75	≤ 0.75
RMSE	56.34	82.30	70.94	51.30	50.49	50.23	41.58	35.03	39.18	46.86	58.59	66.72	65.48	
$PM_{2.5}$ ($\mu g\ m^{-3}$)	**2018**	**2018.01**	**2018.02**	**2018.03**	**2018.04**	**2018.05**	**2018.06**	**2018.07**	**2018.08**	**2018.09**	**2018.10**	**2018.11**	**2018.12**	**Criteria**
OBS	41.61	65.67	57.78	51.66	43.40	35.22	28.98	25.58	25.24	24.93	35.08	50.58	53.72	
PRE	45.21	55.24	53.56	51.26	43.50	35.99	35.24	32.28	33.15	40.59	48.83	62.62	48.27	
MNB	0.49	0.20	0.36	0.39	0.34	0.34	0.46	0.56	0.58	0.96	0.73	0.68	0.35	
MNE	1.01	0.85	0.93	0.91	0.90	0.89	0.97	1.04	1.02	1.38	1.14	1.16	0.95	
MFB	-0.07	-0.26	-0.15	-0.10	-0.14	-0.14	-0.06	-0.03	0.03	0.14	0.10	0.01	-0.18	≤ ±0.6
MFE	0.73	0.75	0.73	0.72	0.73	0.72	0.71	0.71	0.69	**0.77**	0.72	0.75	**0.76**	≤ 0.75
RMSE	50.35	64.24	57.89	54.90	53.40	39.94	35.71	35.15	31.52	45.07	47.01	66.26	56.36	
$PM_{2.5}$ ($\mu g\ m^{-3}$)	**2019**	**2019.01**	**2019.02**	**2019.03**	**2019.04**	**2019.05**	**2019.06**	**2019.07**	**2019.08**	**2019.09**	**2019.10**	**2019.11**	**2019.12**	**Criteria**
OBS	39.85	69.50	58.71	44.61	35.29	31.26	24.40	23.28	21.98	28.43	36.07	43.52	58.76	
PRE	47.11	60.74	58.16	48.85	48.31	35.85	34.22	34.03	35.34	49.57	53.45	48.94	57.22	
MNB	0.66	0.37	0.53	0.52	0.84	0.48	0.72	0.73	0.94	1.08	0.91	0.54	0.40	
MNE	1.14	0.98	1.05	1.04	1.27	1.00	1.16	1.15	1.34	1.40	1.31	1.07	0.94	
MFB	0.02	-0.19	-0.05	-0.06	0.10	-0.08	0.06	0.08	0.15	0.26	0.14	-0.06	-0.11	≤ ±0.6
MFE	0.75	**0.77**	0.74	0.75	0.77	0.74	0.73	0.71	0.75	0.74	**0.76**	**0.76**	0.71	≤ 0.75
RMSE	51.49	74.13	62.13	54.40	49.01	42.44	34.89	36.74	37.99	47.30	53.20	51.35	58.97	
$PM_{2.5}$ ($\mu g\ m^{-3}$)	**2020**	**2020.01**	**2020.02**	**2020.03**	**2020.04**	**2020.05**	**2020.06**	**2020.07**	**2020.08**	**2020.09**	**2020.10**	**2020.11**	**2020.12**	**Criteria**
OBS	36.19	69.20	43.26	35.33	36.20	27.52	22.61	22.25	20.35	24.15	32.86	40.73	59.15	
PRE	44.79	67.05	56.93	45.17	45.18	31.03	28.73	31.01	29.80	44.01	45.07	49.96	63.14	
MNB	0.72	0.58	0.93	0.80	0.67	0.45	0.63	0.73	0.77	1.13	0.79	0.70	0.46	
MNE	1.18	1.11	1.34	1.24	1.08	0.99	1.15	1.21	1.23	1.51	1.24	1.15	0.96	
MFB	0.03	-0.06	0.15	0.08	0.08	-0.09	-0.05	0.00	0.04	0.21	0.08	0.04	-0.06	≤ ±0.6
MFE	0.75	**0.76**	**0.76**	**0.77**	0.71	0.74	0.75	0.74	**0.76**	**0.79**	**0.76**	0.72	0.72	≤ 0.75
RMSE	50.13	75.15	55.76	48.86	56.58	35.15	37.83	35.65	32.25	48.77	46.01	48.22	63.38	
MDA8 O_3 (ppb)	**2015**	**2015.01**	**2015.02**	**2015.03**	**2015.04**	**2015.05**	**2015.06**	**2015.07**	**2015.08**	**2015.09**	**2015.10**	**2015.11**	**2015.12**	**Criteria**
OBS	59.29	50.18	49.86	52.33	59.24	62.21	62.32	62.88	61.96	59.18	59.52	50.59	48.29	
PRE	55.64	40.76	42.50	49.78	56.71	57.73	56.22	62.74	64.35	54.00	52.85	39.08	35.19	
MNB	-0.03	-0.17	-0.13	-0.02	-0.01	-0.03	-0.06	0.04	0.07	-0.06	-0.08	-0.20	-0.24	
MNE	0.26	0.24	0.23	0.22	0.23	0.25	0.27	0.30	0.28	0.26	0.24	0.28	0.29	
MFB	-0.09	-0.23	-0.18	-0.07	-0.05	-0.09	-0.12	-0.03	0.01	-0.12	-0.13	-0.29	-0.33	≤ ±0.6
MFE	0.27	0.30	0.28	0.23	0.23	0.26	0.29	0.29	0.26	0.28	0.26	0.36	0.38	≤ 0.75
RMSE	20.48	18.25	16.83	16.25	18.58	20.72	22.36	23.59	21.68	19.95	19.19	20.44	23.93	
MDA8 O_3 (ppb)	**2016**	**2016.01**	**2016.02**	**2016.03**	**2016.04**	**2016.05**	**2016.06**	**2016.07**	**2016.08**	**2016.09**	**2016.10**	**2016.11**	**2016.12**	**Criteria**
OBS	59.14	46.87	48.71	54.25	58.18	63.04	64.42	62.73	60.98	62.57	53.20	50.42	49.29	
PRE	55.12	38.61	43.28	49.69	53.96	55.29	60.40	65.14	61.15	58.09	45.61	41.43	38.50	
MNB	-0.04	-0.16	-0.10	-0.06	-0.04	-0.08	-0.03	0.07	0.04	-0.05	-0.12	-0.16	-0.20	
MNE	0.25	0.22	0.20	0.21	0.24	0.25	0.26	0.30	0.28	0.26	0.25	0.26	0.25	
MFB	-0.10	-0.21	-0.14	-0.10	-0.08	-0.14	-0.09	0.01	-0.02	-0.10	-0.18	-0.23	-0.27	≤ ±0.6
MFE	0.27	0.27	0.23	0.23	0.25	0.28	0.28	0.28	0.27	0.28	0.29	0.32	0.31	≤ 0.75
RMSE	19.87	16.43	13.66	15.49	18.13	21.33	21.26	23.59	21.13	21.00	17.85	17.98	17.00	
MDA8 O_3 (ppb)	**2017**	**2017.01**	**2017.02**	**2017.03**	**2017.04**	**2017.05**	**2017.06**	**2017.07**	**2017.08**	**2017.09**	**2017.10**	**2017.11**	**2017.12**	**Criteria**

OBS	60.80	48.12	50.35	51.91	59.40	68.16	69.98	67.33	61.86	61.54	54.46	52.76	49.88	
PRE	55.25	40.50	46.59	47.73	53.63	59.33	62.87	66.38	61.19	54.12	47.89	40.99	39.03	
MNB	-0.07	-0.15	-0.06	-0.06	-0.07	-0.09	-0.07	0.02	0.02	-0.09	-0.10	-0.20	-0.20	
MNE	0.24	0.21	0.21	0.19	0.21	0.23	0.24	0.27	0.27	0.26	0.23	0.27	0.24	
MFB	-0.12	-0.19	-0.10	-0.09	-0.11	-0.14	-0.12	-0.04	-0.04	-0.15	-0.15	-0.27	-0.26	≤ ±0.6
MFE	0.25	0.25	0.23	0.20	0.23	0.25	0.26	0.26	0.27	0.29	0.26	0.33	0.29	≤ 0.75
RMSE	19.17	13.74	13.98	13.32	16.78	20.93	21.57	22.43	21.60	20.74	16.29	18.94	16.48	
MDA8 O_3 (ppb)	**2018**	**2018.01**	**2018.02**	**2018.03**	**2018.04**	**2018.05**	**2018.06**	**2018.07**	**2018.08**	**2018.09**	**2018.10**	**2018.11**	**2018.12**	**Criteria**
OBS	60.54	48.33	48.05	55.41	62.06	64.07	72.26	63.03	63.00	56.83	57.14	49.86	47.90	
PRE	55.38	43.07	42.89	52.22	56.56	57.74	62.93	62.09	60.37	51.57	49.90	43.28	41.16	
MNB	-0.06	-0.10	-0.10	-0.04	-0.06	-0.07	-0.09	0.01	-0.01	-0.07	-0.10	-0.11	-0.12	
MNE	0.23	0.20	0.20	0.20	0.21	0.23	0.25	0.26	0.26	0.25	0.21	0.24	0.23	
MFB	-0.11	-0.14	-0.14	-0.07	-0.10	-0.11	-0.14	-0.04	-0.07	-0.12	-0.14	-0.17	-0.18	≤ ±0.6
MFE	0.25	0.23	0.23	0.21	0.22	0.24	0.27	0.26	0.27	0.27	0.23	0.28	0.28	≤ 0.75
RMSE	18.84	14.17	12.73	14.52	17.29	19.37	23.50	21.13	21.12	18.66	16.09	15.53	16.75	
MDA8 O_3 (ppb)	**2019**	**2019.01**	**2019.02**	**2019.03**	**2019.04**	**2019.05**	**2019.06**	**2019.07**	**2019.08**	**2019.09**	**2019.10**	**2019.11**	**2019.12**	**Criteria**
OBS	60.35	49.19	47.35	50.70	56.28	63.01	68.10	64.89	62.43	65.82	57.87	56.91	49.06	
PRE	57.41	45.07	43.30	48.77	56.18	58.68	63.16	66.22	62.29	61.09	52.78	46.62	44.62	
MNB	-0.02	-0.07	-0.07	-0.02	0.02	-0.04	-0.04	0.05	0.03	-0.05	-0.06	-0.16	-0.08	
MNE	0.23	0.19	0.24	0.19	0.22	0.21	0.24	0.27	0.26	0.22	0.23	0.22	0.18	
MFB	-0.07	-0.11	-0.13	-0.05	-0.02	-0.08	-0.09	-0.01	-0.03	-0.10	-0.11	-0.20	-0.11	≤ ±0.6
MFE	0.24	0.22	0.27	0.20	0.22	0.22	0.25	0.26	0.26	0.24	0.26	0.26	0.20	≤ 0.75
RMSE	18.14	12.47	14.76	13.07	15.82	17.25	20.29	22.27	20.75	18.41	18.04	17.13	12.18	
MDA8 O_3 (ppb)	**2020**	**2020.01**	**2020.02**	**2020.03**	**2020.04**	**2020.05**	**2020.06**	**2020.07**	**2020.08**	**2020.09**	**2020.10**	**2020.11**	**2020.12**	**Criteria**
OBS	57.59	46.60	47.03	50.00	58.75	61.65	65.01	61.46	59.19	59.68	53.87	52.46	47.77	
PRE	54.97	43.26	44.51	50.00	56.85	58.20	60.30	61.19	60.39	56.15	47.22	45.19	40.93	
MNB	-0.02	-0.06	-0.04	0.01	-0.01	-0.02	-0.04	0.02	0.05	-0.04	-0.10	-0.12	-0.13	
MNE	0.22	0.24	0.21	0.19	0.18	0.22	0.24	0.26	0.27	0.23	0.22	0.20	0.22	
MFB	-0.07	-0.11	-0.09	-0.02	-0.03	-0.06	-0.09	-0.03	-0.01	-0.09	-0.15	-0.16	-0.18	≤ ±0.6
MFE	0.23	0.26	0.23	0.19	0.18	0.23	0.25	0.26	0.26	0.24	0.25	0.23	0.26	≤ 0.75
RMSE	17.21	14.68	13.20	13.00	14.03	18.08	19.90	20.70	20.31	17.42	16.17	13.90	13.99	

Table S2. Summary of previous studies reporting observed monthly OC concentrations across Chinese cities.

Site	Latitude (°N)	Longitude (°E)	Observation Year	Reference
Hefei	31.86	117.26	2014	[2]
Dongguan	23.06	113.75	2010, 2018	[3,4]
Foshan	23.03	113.14	2010	[3,4]
Karamay	44.32	84.88	2015	[5,6]
Beijing	39.9	116.41	2010, 2012, 2013, 2014, 2015, 2016, 2017	[7,8]
Nanjing	32.02	118.73	2011, 2012, 2013, 2014, 2015, 2016, 2017, 2018	[9]

Nanchang	28.7	115.97	2013, 2015	[10]
Tianjin	39.08	117.2	2006, 2009, 2010, 2017	[11,12]
Guangzhou	23.13	113.26	2010, 2012, 2013, 2015	[3]
Chengdu	30.67	104.02	2010, 2011, 2013, 2015, 2017, 2019	[13–15]
Xinxiang	35.32	113.91	2015	[16–18]
Tai’an	36.14	117.06	2015	[10,19]
Haikou	20.0	110.34	2015	[20]
Shenzhen	22.58	114.13	2010	[3,4]
Zhuhai	22.35	113.58	2010	[3,4]
Heze	35.25	115.46	2015, 2016	[21]
Yuncheng	35.04	111.02	2015	[22]
Handan	36.58	114.51	2013, 2014, 2015, 2016, 2017, 2018	[23,24]
Zhengzhou	34.75	113.61	2014, 2015, 2019, 2020	[16–18]
Jinhua	29.1	119.57	2015	[25]
Shenyang	41.81	123.44	2015, 2017	[26]
Xi’an	34.23	109.01	2012, 2013, 2014, 2015, 2016, 2017	[27]
Urumchi	43.82	87.58	2013	-
Baoding	39.13	115.67	2014	-
Nanchong	30.82	106.07	2017	[28]
Xiamen	24.48	118.09	2013, 2014	[29]
Lvliang	37.74	111.33	2017	[30]
Jiaxing	30.82	120.87	2019	[31]
Dalian	38.95	121.62	2013	[32]
Hangzhou	30.27	120.16	2012, 2013	[33]
Yulin	38.29	109.73	2013	[2]
Wuhan	30.59	114.31	2015	[34]
Jinan	36.67	117.06	2014, 2019	[35,36]
Weinan	34.73	109.53	2016	[37]
Baise	23.89	106.63	2016	[38]
Panjin	41.13	122.04	2016	[39]
Shijiazhuang	38.06	114.54	2017	[40]
Xining	36.65	101.71	2014	[2]
Jinchang	38.52	102.19	2013	[41]

Yinchuan	38.50	106.14	2014	[2]
Jinzhou	41.06	121.12	2018	[42]
Yangquan	37.85	113.61	2018, 2019	[43]
Qingdao	36.07	120.38	2013, 2014	[35]
Hainan Tibetan	36.28	100.90	2009	[44]

Table S3. Comparison of PBrC light absorption between previous literatures and this study.

Site	Location	Sampling period	PBrC light absorption (370 nm) (Mm^{-1})		Reference
			Previous study	This study	
Guanzhong	34.12°N, 108.62°E	December 2015 – January 2016	8.6	8.8	[45]
Shanghai	31.73°N, 121.22°E	December 2019 – January 2020	4.6	6.8	[46]
Beijing	39.97°N, 116.37°E	September 2017 – February 2018	23.6	12.6	[47]
Beijing	39.97°N, 116.37°E	March 2018 – February 2019	16.7	11.5	[47]
Beijing	39.97°N, 116.37°E	March 2019 – February 2020	10.4	10.9	[47]
Beijing	39.97°N, 116.37°E	March 2020 – November 2020	7.4	7.8	[47]
Ngari	34.12°N, 108.62°E	March 2020 – July 2020	1.2	0.2	[48]
Wuhan	30.53°N, 114.39°E	January 2020 – April 2020	2.1	13.1	[49]
Nanjing	32.50°N, 80.10°E	January 2020 – March 2020	9.3	11.4	[50]
Xi'an	34.27°N, 108.90°E	16 December 2016 – 15 January 2017	27.3	20.4	[51]
Hong Kong	22.32°N, 114.15°E	16 December 2016 – 15 January 2017	1.5	7.9	[51]
Qinghai Lake	37.04°N, 99.74°E	August 2018 – September 2019	1.9	0.4	[48]
Beiluhe	34.82°N, 92.93°E	September 2018 – July 2019	0.2	0.1	[48]
Hua Mount	34.48°N, 110.08°E	August 2018	1.9	1.7	[52]
Lijiang	26.70°N, 100.03°E	14 March 2018 – 13 May 2018	2.9	1.4	[53]
Harbin	45.74°N, 126.73°E	20 November 2019 – 25 December 2019	16.9	12.1	[54]
Beijing	39.97°N, 116.36°E	20 November 2019 – 25 December 2019	7.1	15.3	[54]
Xi'an	34.23°N, 108.88°E	20 November 2019 – 25 December 2019	13.6	17.7	[54]
Shanghai	31.18°N, 121.59°E	20 November 2019 – 25 December 2019	2.4	7.6	[54]
Wuhan	30.53°N, 114.39°E	20 November 2019 – 25 December 2019	3.0	14.9	[54]
Guangzhou	23.12°N, 113.35°E	20 November 2019 – 25 December 2019	2.5	8.2	[54]
Nanning	22.83◦N, 108.39◦E	March 2020 – December 2020	6.2	3.3	[55]
Shaoguan	24.70°N, 112.90°E	18 November 2020 – 5 December 2020	1.1	3.3	[56]
Sanya	18.30°N, 109.52°E	12 April 2017 – 14 May 2017	2.5	1.1	[57]
Zhengzhou	34.81°N, 113.72°E	6 December 2019 – 9 December 2019	6.9	14.2	[58]

Huludao	40.48°N, 120.78°E	13 October 2020 – 31 December 2020	3.0	3.9	[59]
Hainan Tibetan	36.28°N, 100.90°E	3 January 2020 – 31 March 2020	2.5	0.8	[60]
Anshan	41.27°N, 122.83°E	January 2017 – August 2017	29	7.4	[61]
Binzhou	37.38°N, 118.01°E	January 2017 – August 2017	18.4	6.8	[61]
Beijing(Changping)	39.97°N, 116.37°E	January 2017 – August 2017	29.4	11.3	[61]
Diqing	27.82°N, 99.70°E	January 2017 – August 2017	0.1	0.4	[61]
Hainan Tibetan	36.28°N, 100.62°E	January 2017 – August 2017	0.1	0.6	[61]
Fushun	41.88°N, 123.93°E	January 2017 – August 2017	11.4	5.9	[61]
Lanzhou	36.06°N, 103.84°E	January 2017 – August 2017	7	2.9	[61]
Hangzhou(Lin'an)	30.24°N, 119.72°E	January 2017 – August 2017	2.2	4.0	[61]
Lu'an	31.77°N, 116.48°E	January 2017 – August 2017	4.5	6.8	[61]
Nanning	22.83°N, 108.39°E	January 2017 – August 2017	8.2	3.9	[61]
Shanghai(Pudong)	31.73°N, 121.59°E	January 2017 – August 2017	1.3	5.4	[61]
Tongliao	43.62°N, 122.27°E	January 2017 – August 2017	5.7	2.1	[61]
Harbin(Wuchang)	45.74°N, 126.73°E	January 2017 – August 2017	16.1	8.8	[61]
Xi'an	34.23°N, 108.88°E	January 2017 – August 2017	1.9	11.8	[61]
Xiangyang	32.08°N, 112.13°E	January 2017 – August 2017	6.2	7.5	[61]
Xilinhot	43.95°N, 116.07°E	January 2017 – August 2017	0.7	1.5	[61]
Yichang	30.70°N, 111.28°E	January 2017 – August 2017	12.2	4.2	[61]

Table S4 Emission factor of PBrC and origin imaginary part of complex refractive index (k) in this study.

	AGRI	BLDG	INDC	INDP	FUEL	WSTE	POWR	TRAN	WLDF
Factor	0.5	0.5	0.3	0.03	0.03	0.3	0.16	0.05	0.1
k 294 nm	0.101	0.118	0.118	0.118	0.118	0.118	0.118	0.118	0.101
k 303 nm	0.101	0.118	0.118	0.118	0.118	0.118	0.118	0.118	0.101
k 310 nm	0.101	0.118	0.118	0.118	0.118	0.118	0.118	0.118	0.101
k 316 nm	0.101	0.118	0.118	0.118	0.118	0.118	0.118	0.118	0.101
k 333 nm	0.100	0.117	0.117	0.117	0.117	0.117	0.117	0.117	0.100
k 381 nm	0.076	0.089	0.089	0.089	0.089	0.089	0.089	0.089	0.076
k 607 nm	0.023	0.016	0.016	0.016	0.016	0.016	0.016	0.016	0.023

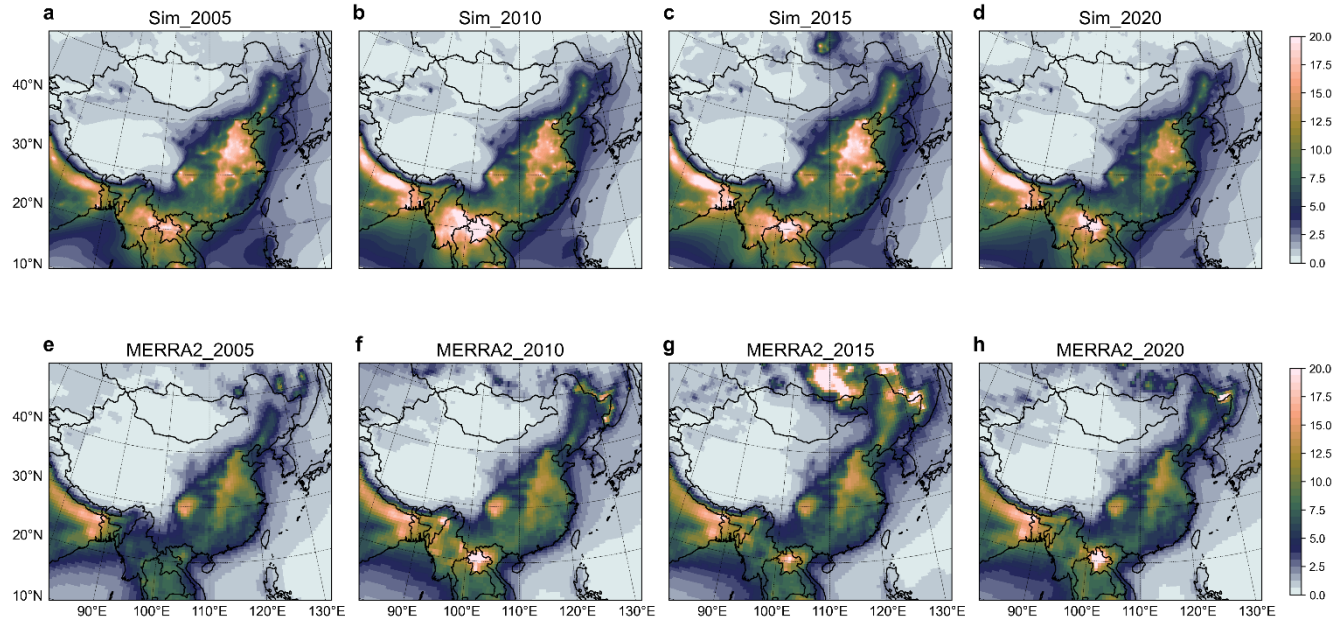

Figure S1. Comparison of annual OC concentrations between simulations and MERRA-2 data. (a-d) Simulated annual OC concentrations for 2005, 2010, 2015, and 2020. (e-f) Annual OC concentrations from MERRA-2 data for the same years.

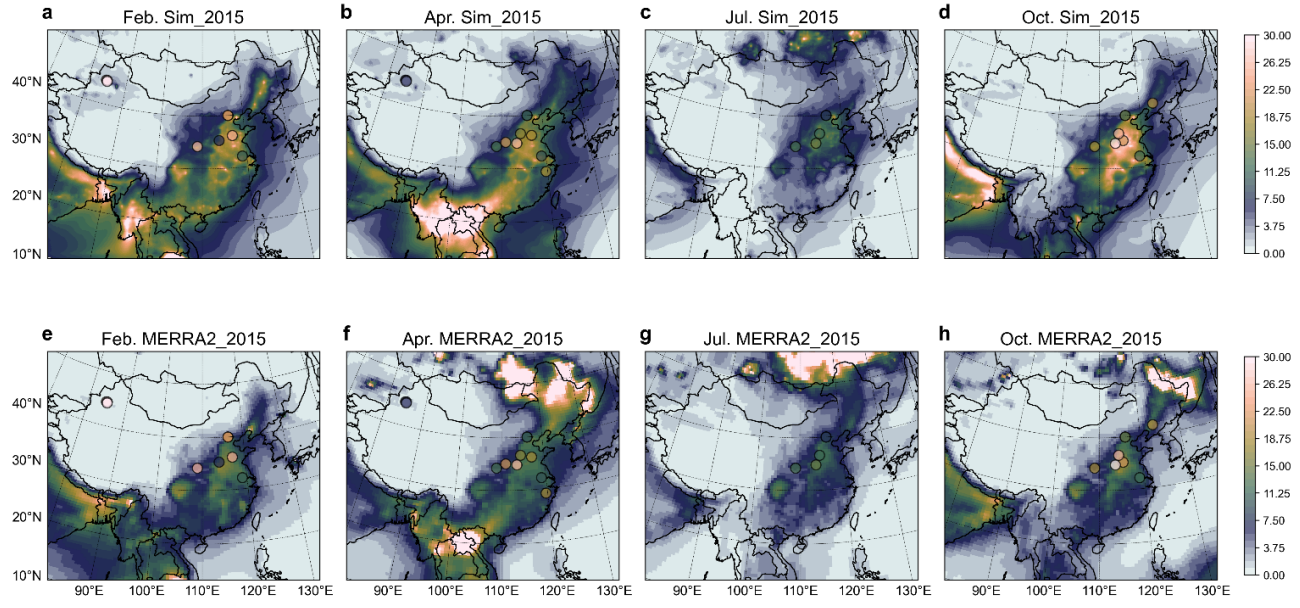

Figure S2. Comparison of monthly OC concentrations between simulations and MERRA-2 data in 2015. (a,e) February, 2015; (b,f) April, 2015; (c,g) July, 2015; (d,h) October, 2015. Dots represent observed OC concentrations from previous studies (Table S2).

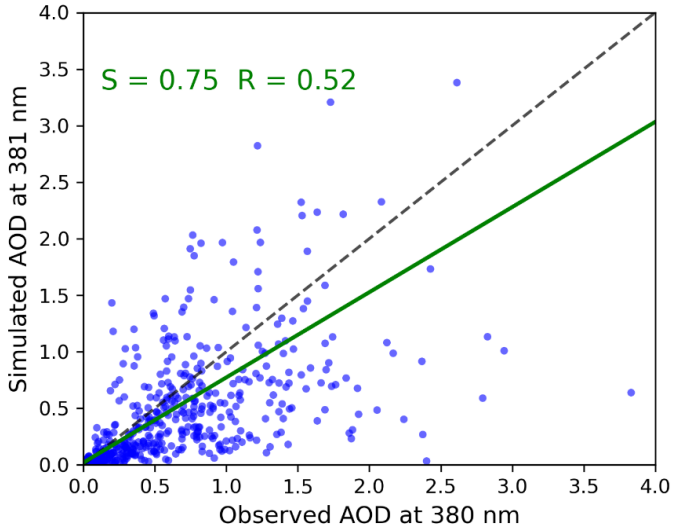

Figure S3. Validation of AOD at short wavelengths. The slopes (S) of the regression lines, and the Pearson correlation coefficients (R) are shown as insets. The dashed lines indicate the 1:1 line.

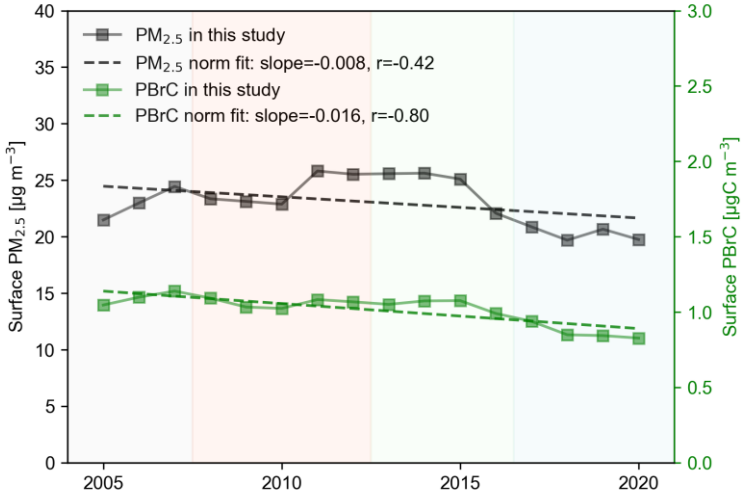

Figure S4. Temporal changes in annual $PM_{2.5}$ and PBrC surface concentrations in China. Dotted lines indicate results of normalized linear regressions.

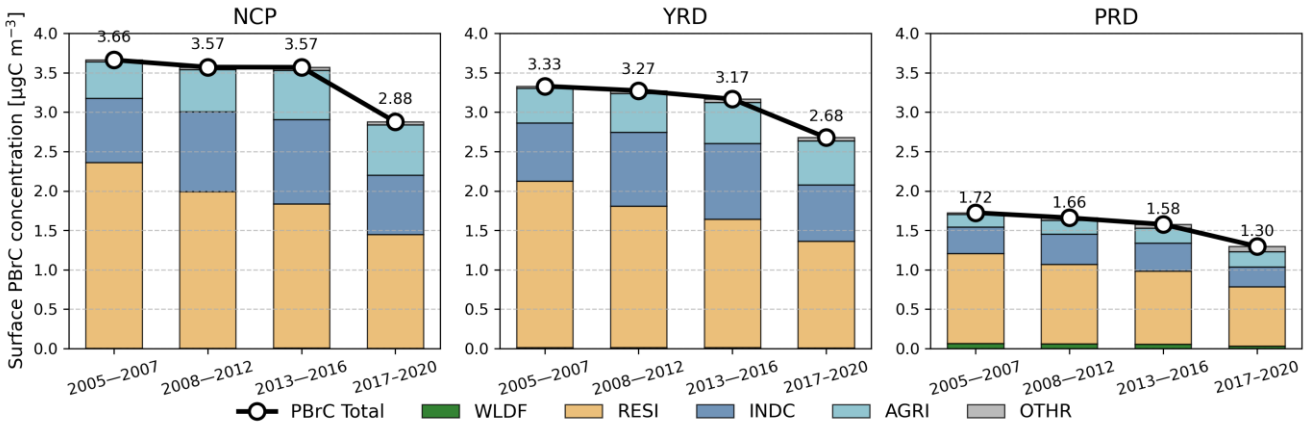

Figure S5. Temporal variations in source contributions to surface PBrC in the NCP, YRD, and PRD regions.

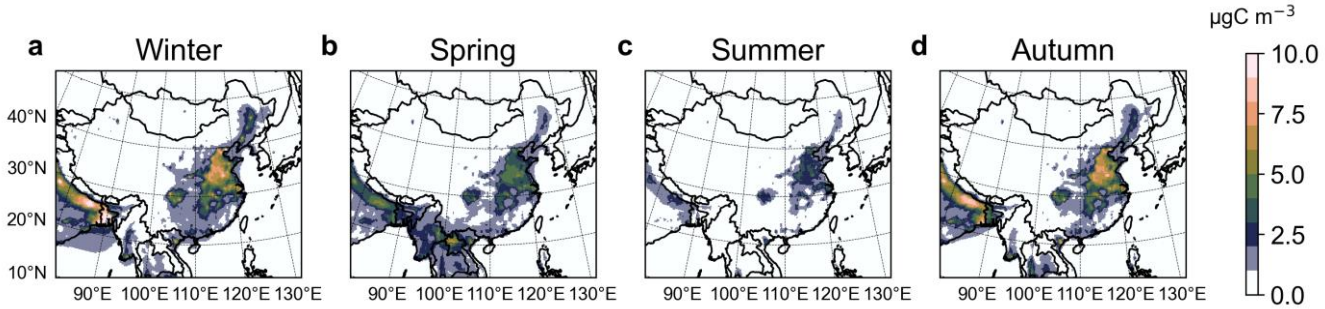

Figure S6. Multi-year mean distributions of simulated PBrC. (a) Winter (December, January, and February); (b) Spring (March, April, and May); (c) Summer (June, July, and August); (d) Autumn (September, October, and November).

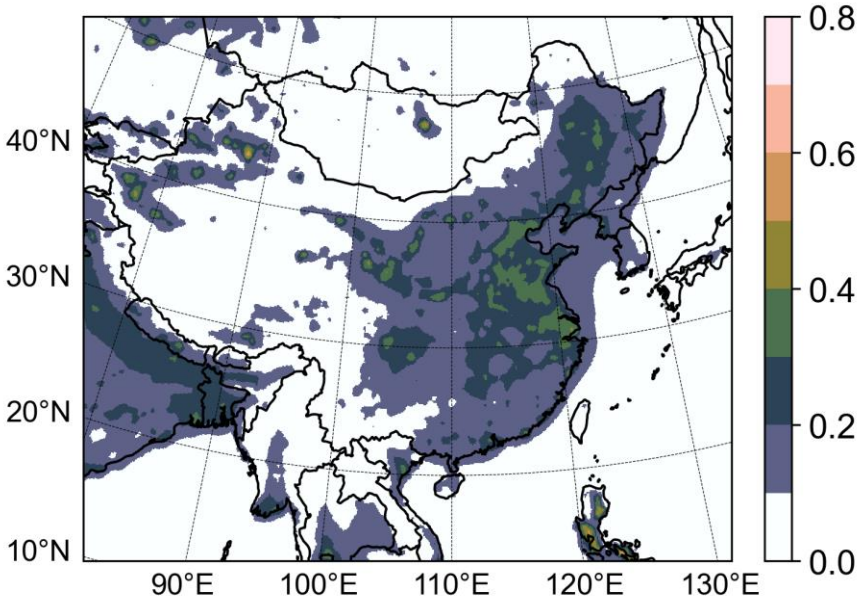

Figure S7. Simulated multi-year mean distribution of the PBrC to OC ratio.

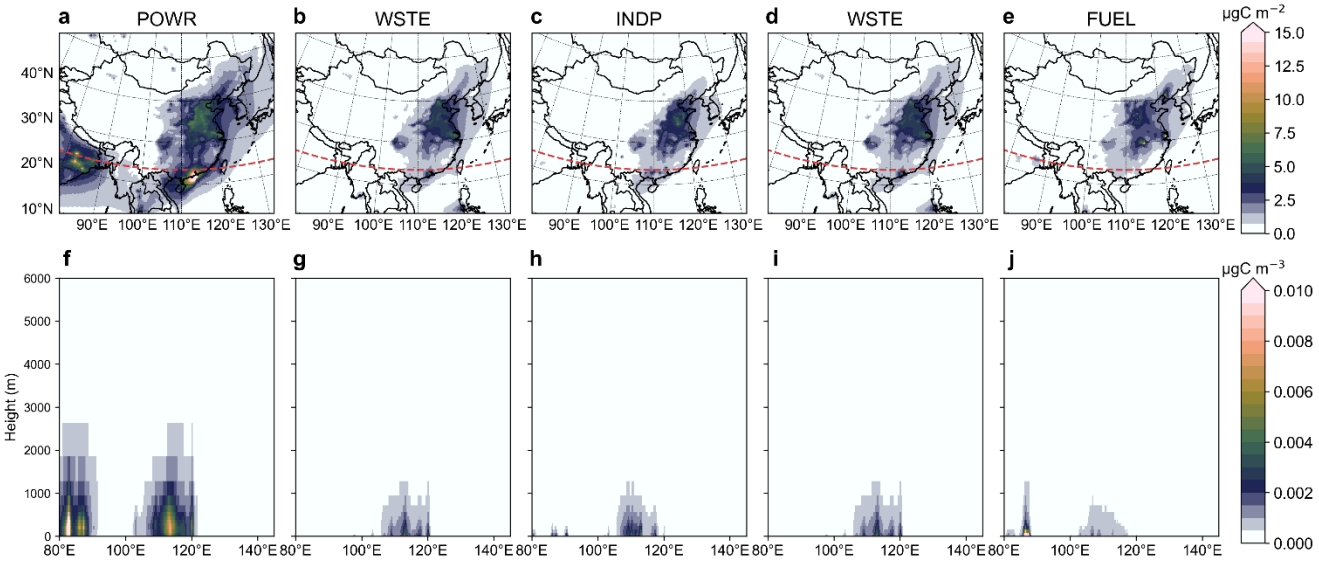

Figure S8. Column concentrations and vertical cross-sections of PBrC in 2010. (a-e) Column contributions from power plants (POWR), transport (TRAN), industrial processes (INDP), waste (WSTE), and fuel exploitation (FUEL) sources. (e-f) Vertical cross-sections of PBrC concentrations along 23.5°N from power plants, transport, industrial processes, waste, and fuel exploitation sources. Red dashed lines mark 23.5°N.

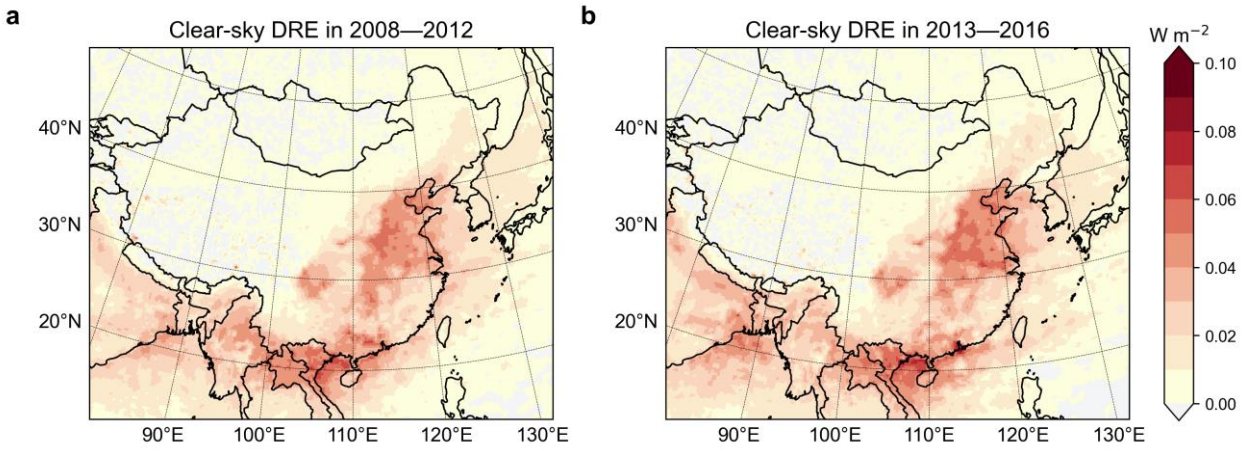

Figure S9. Spatial distribtuions of PBrC DRE in 2008–2012 and 2013–2016.

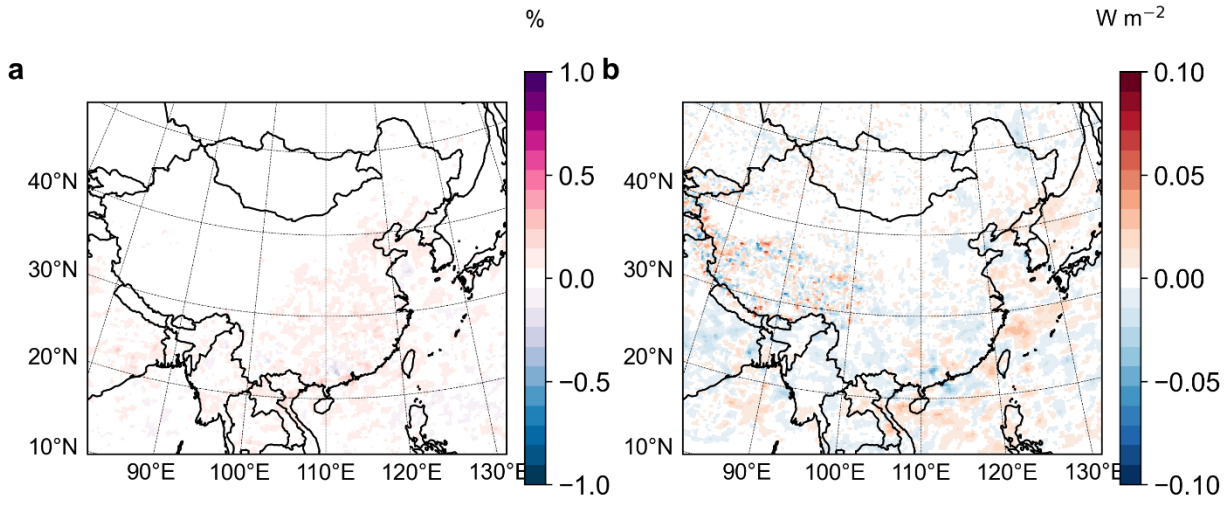

Figure S10. Impacts of PBrC aging on O_3 concentrations and DRE in 2010.

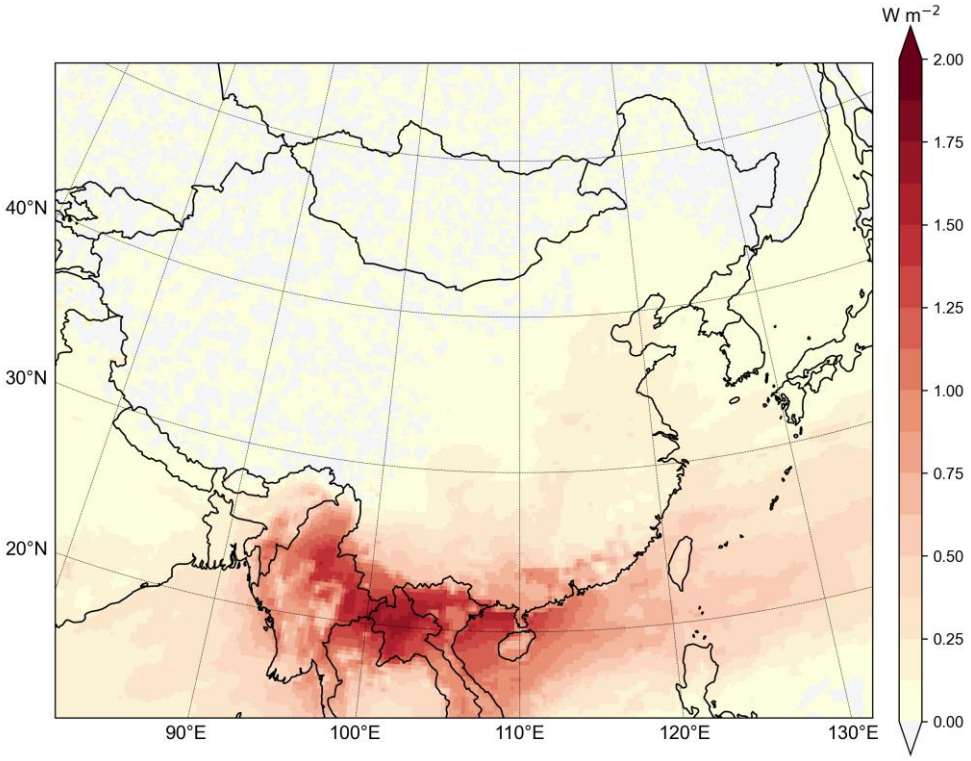

Figure S11. PBrC DRE in March 2010 after adjusting k value.

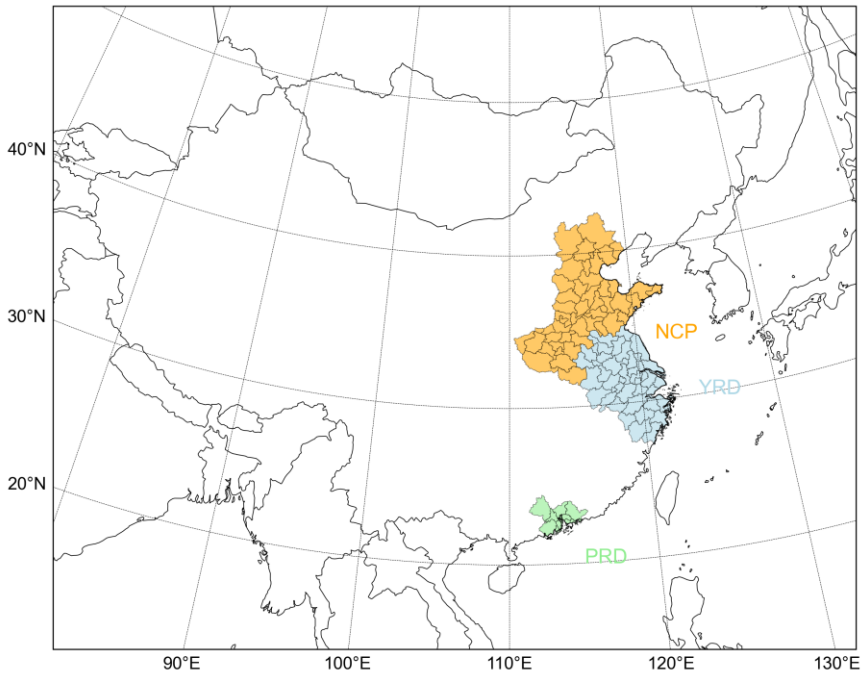

Figure S12. Model domain in this study.

References

1. EPA, U. Guidance on the Use of Models and Other Analyses for Demonstrating Attainment of Air Quality Goals for Ozone, $PM_{2.5}$, and Regional Haze. Office of Air and Radiation/Office of Air Quality Planning and Standards, Research Triangle Park, NC, USA (2007).
2. Liu, S. et al. Tracking Daily Concentrations of PM2.5 Chemical Composition in China since 2000. Environ. Sci. Technol. **56**, 16517–16527 (2022).
3. Yang, Y.; Qu, Q.; Liu, S.; Li, X.; Zhong, P.; Tao, J. Chemical Compositions in PM2.5 and Its Impact on Visibility in Summer in Pear River Delta， China. Environ. Sci. 2015, 36 (8), 2758–2767. https://doi.org/10.13227 /j.hjkx.2015.08.005. (in Chinese).

4. Zhang, X.; Zhao, X.; Ying, R.; Ji, G.; Han, C.; Kong, L.; Feng, Y.; Shan, Y.; Lin, Y. Characteristics and Source Apportionments of Carbonaceous Components in Atmospheric Fine Particles in Guangzhou. J. Ecol. Rural Environ. 2018, 34 (7), 659–666. https://doi.org/10.11934/j.issn.1673－4831.2018.07.012. (in Chinese).
5. Yusan, T. Chemical Characteristics, Source Apportionment and Health Risks Assessment of PM2.5 in Dushanzi During 2015-2016, Xinjiang University, 2018. (in Chinese).
6. Shen, H.; Dilinuer, T.; Wang, X.; Ding, X.; Abulikemu, A.; Malikezhati, M.; Yalikunjiang, T.; Yusan, T.; Liu, W.; Han, Y. Formation Mechanism of Water-Soluble Inorganic Ions in PM2．5 in Dushanzi Petrochemical District，Xinjiang. Environ. Chem. 2018, 37 (11), 2443–2451. https://doi.org/10.7524/j.issn.0254-6108.2018010803. (in Chinese).
7. Liu, Y.-J.; Zhang, T.-T.; Liu, Q.-Y.; Zhang, R.-J.; Sun, Z.-Q.; Zhang, M.-G. Seasonal Variation of Physical and Chemical Properties in TSP, PM10 and PM2. 5 at a Roadside Site in Beijing and Their Influence on Atmospheric Visibility. Aerosol Air Qual. Res. 2014, 14 (3), 954–969. https://doi.org/Seasonal Variation of Physical and Chemical Properties in TSP, PM10 and PM2.5 at a Roadside Site in Beijing and Their Influence on Atmospheric Visibility.
8. Song, S.; Wu, Y.; Jiang, J.; Yang, L.; Cheng, Y.; Hao, J. Chemical Characteristics of Size-Resolved PM2. 5 at a Roadside Environment in Beijing, China. Environ. Pollut. 2012, 161, 215–221. https://doi.org/https://doi.org/10.1016/j.envpol.2011.10.014.
9. Ding, A.; Huang, X.; Nie, W.; Chi, X.; Xu, Z.; Zheng, L.; Xu, Z.; Xie, Y.; Qi, X.; Shen, Y.; Sun, P.; Wang, J.; Wang, L.; Sun, J.; Yang, X. Q.; Qin, W.; Zhang, X.; Cheng, W.; Liu, W.; Pan, L.; Fu, C. Significant Reduction of PM2.5 in Eastern China Due to Regional-Scale Emission Control: Evidence from SORPES in 2011-2018. Atmos. Chem. Phys. 2019, 19 (18), 11791–11801. https://doi.org/10.5194/acp-19-11791-2019.
10. Feng, T.; Cai, Y.; Li, Z.; Yang, F.; Wang, F. Seasonal Variation and Source Apportionment of PM2.5 Carbonaceous Aerosol in a Typical Urban Area of Chongqing. Acta Sci. Circumstantiae 2021, 41 (5), 1703–1717. https://doi.org/10.13671/j.hjkxxb.2020.0446. (in Chinese).
11. Yao, Q.; Zhao, P.; Han, S.; Liu, A. Pollution Character of Carbonaceous Aerosol in PM2.5 in Tianjin City. Environ. Chem. 2014, 33 (3), 404–410. https://doi.org/10.7524/j.issn.0254-6108.2014.03.004. (in Chinese).

12. Li, P.; Gao, J.; Xiao, Z.; Bi, W.; Li, Y. Characteristics of Water-Soluble Ions of PM2.5 in Tianjin. Environ. Sci. Manag. 2021, 46 (3), 95–99. https://doi.org/10.3969/j.issn.1673-1212.2021.03.023. (in Chinese).
13. Wang, Q.; Tao, J.; Ren, P.; Shen, Z.; Luo, L.; Tang, X. Chemical Composition of PM2.5 and Its Impact on Visibility at Chengdu in 2010 Winter. J. Earth Environ. 2012, 3 (5), 1104–1108. https://doi.org/10.7515/JEE201205014. (in Chinese).
14. Zhang, J.; Lin, Y.; Qiao, Y.; Yang, H.; Ye, Z. Character of Carbonaceous Aerosol in PM2.5 during Summer-Autumn Period in Southwest Suburb of Chengdu. Environ. Eng. 2017, 35 (10), 100–104. https://doi.org/10.13205/j.hjgc.201710021. (in Chinese).
15. Yuan, X.; Zhu, Y.; Liao, R.; Li, S. Water-Soluble Ions Characteristics of Fine Particulate Matter during Heavy Pollution Period in Chengdu. Sichuan Environ. 2017, 36 (1001–3644), 28–31. https://doi.org/10.14034/j.cnki.schj.2017.s1.006. (in Chinese).
16. Feng J, et al. (2016) Chemical composition and source apportionment of PM2.5 during Chinese Spring Festival at Xinxiang, a heavily polluted city in North China: Fireworks and health risks. Atmos. Res. 182:176-188.
17. Wang, S.; Fan, X.; He, B.; Zhang, R.; Wang, L. Chemical Composition Characteristics of PM2.5 in Henan Province during the Spring Festival and COVID-19 Outbreak. China Environ. Sci. 2020, 40 (12), 5115–5123. https://doi.org/10.3969/j.issn.1000-6923.2020.12.002. (in Chinese).
18. Wang, Q.; Jiang, N.; Yin, S.; Li, X.; Yu, F.; Guo, Y.; Zhang, R. Carbonaceous Species in PM2. 5 and PM10 in Urban Area of Zhengzhou in China: Seasonal Variations and Source Apportionment. Atmos. Res. 2017, 191, 1–11. https://doi.org/https://doi.org/10.1016/j.atmosres.2017.02.003.
19. Mei, R.; Sui, B. Chemical Composition Characteristics of PM2.5 in Taishan Scenic Area during Winter and Spring. Environ. Pollut. Control 2018, 40 (1), 84–87. https://doi.org/10.15985/j.cnki.1001-3865.2018.01.018. (in Chinese).
20. Liu, B.; Li, T.; Yang, J.; Wu, J.; Wang, J.; Gao, J.; Bi, X.; Feng, Y.; Zhang, Y.; Yang, H. Source Apportionment and a Novel Approach of Estimating Regional Contributions to Ambient PM2. 5 in Haikou, China. Environ. Pollut. 2017, 223, 334–345. https://doi.org/https://doi.org/10.1016/j.envpol.2017.01.030.

21. Liu, Z. J.; Wu, J. H.; Zhang, Y. F.; Liang, D. N.; Ma, X.; Liu, B. S.; Feng, Y. C.; Zhang, Q. X. Seasonal Variation of Carbon Fractions in PM2. 5 in Heze. Environ. Sci. 2017, 38 (12), 4943–4950. https://doi.org/10.13227/j.hjkx.201704296. (in Chinese).
22. Wu, Y. Chemical Composition Characteristics of Fine Particulate Matter (PM2.5) in Yuncheng, Taiyuan University of Technology, 2017. (in Chinese).
23. Ma, X.; Wang, L.; Ma, S.; Wei, Z.; Zhang, C.; Zheng, A. Spatial and Temporal Distribution and Source Analysis of Components in PM2.5， Handan. Environ. Chem. 2017, 36 (9), 1932–1940. https://doi.org/10.7524/j.issn.0254-6108.2017020102. (in Chinese).
24. Zhai, S.; Jacob, D. J.; Wang, X.; Liu, Z.; Wen, T.; Shah, V.; Li, K.; Moch, J. M.; Bates, K. H.; Song, S. Control of Particulate Nitrate Air Pollution in China. Nat. Geosci. 2021, 14 (6), 389–395. https://doi.org/https://doi.org/10.1038/s41561-021-00726-z.
25. Zhou, H.; Wang, Y.; Xu, B.; Feng, J.; Wang, W.; Chang, Y.; Zhang, M.; Wu, M. Pollution Characteristics of PM2.5 and Its Carbonaceous Species in Jinhua. Environ. Sci. Technol. 2018, 41 (10), 192–197. https://doi.org/10.19672/j.cnki.1003-6504.2018.10.027. (in Chinese).
26. Zhao, B. The Research of PM2.5 Pollution Rules and Distribution Characteristics of Chemical Components in Shenyang's Atmosphere, Liaoning University, 2017. (in Chinese).
27. Zhang, Y.; Wang, H.; Xiao, H.; Lu, H.; Zhang, Z.; Zheng, N.; Luo, L. Winter Spatial Distribution and Source Apportionment of Water-Soluble Ions in PM2.5, Northeast Asia. China Environ. Sci. 2019, 39 (6), 2291–2298. https://doi.org/10.19674/j.cnki.issn1000-6923.2019.0272. (in Chinese).
28. Guo, J. Chemical Compositions and Source Apportinment of Atmospheric PM2.5 in Key Cities of Northeastern Sichuan,China, China West Normal University, 2020. (in Chinese).
29. Hu, Q. Chemical Composition Characteristics and Source Apportionment of Atmospheric PM2.5 in Xiamen City, Huaqiao University, 2016. (in Chinese).
30. Yang, G. Study on Pollution Characteristics of Water-Soluble Ions and Carbonaceous Components in PM2.5 in Typical Coking Pollution Areas, Taiyuan University of Science and Technology, 2020. (in Chinese).

31. Zhang, Y.; Li, L.; Song, L.; Wang, F.; Zhao, H.; Wu, W.; Tang, Q.; Pan, C.; Chen, H. Chemical Components Characteristic and Source Apportionment of PM2.5 during Winter in Jiaxing. Environ. Chem. 2021, 40 (3), 754–764. https://doi.org/10.7524/j.issn.0254-6108.2020062303. (in Chinese).
32. Huijun, F.; Deyu, J.; Dan, L.; Shuyi, M.; Jie, X. A Study on the Concentration Characteristics of Carbonaceous Matter in PM2.5 in Dalian Ambient Air. J. Environ. Manag. Coll. China-EMCC 2014, 24 (5), 0–4. https://doi.org/10.13358/j.issn.1008-813x.2014.05.14. (in Chinese).
33. Du, R.; Qi, B.; Xu, H.; He, J. Characteristics of Carbon Aerosol Pollution in PM2.5 in Hangzhou. Environ. Chem. 2013, 1 (12), 2400–2401. https://doi.org/Characteristics of carbon aerosol pollution in PM2.5 in Hangzhou. (in Chinese).
34. Cheng, Y.; Wu, J.; Bi, X.; Yang, J.; Liu, B.; Dai, Q.; Li, P.; Yu, J.; Feng, Y. Characteristics and Source Apportionment of Water-Soluble Ions in Ambient PM2.5 in Wuhan， China. Acta Sci. Circumstantiae 2019, 39 (1), 189–196. https://doi.org/10.13671/j.hjkxxb.2018.0329. (in Chinese).
35. Gao, S.; Fan, G.; Hou, L. Pollution Characteristics of Carbon Components in PM2.5 in Coastal and Inland Cities of Shandong Province. Proc. 2016 Annu. Conf. Chinese Soc. Environ. Sci. (Volume 3) 2016, 1 (1), 66–71. (in Chinese).
36. Wei, X.; Liu, G.; Yan, X.; Hao, S.; Zhang, G.; Liang, D.; Wang, P. Characteristics of PM2.5 Number Concentrations and Compositions during Heavy Air Pollution Events in Ji'nan. Ecol. Environ. Sci. 2020, 29 (9), 1847–1854. https://doi.org/10.16258/j.cnki.1674-5906.2020.09.017. (in Chinese).
37. Li, J.; Li, J.; Wu, C.; Cao, C.; Wu, Y.; Liu, L.; Han, J.; Wang, G. Comparison on the Chemical Composition of PM2 .5 in the Urban and Rural Regions of Guanzhong Plain, China. China Environ. Sci. 2018, 38 (12), 4415–4425. https://doi.org/10.3969/j.issn.1000-6923.2018.12.003. (in Chinese).
38. Zhang, D.; Chen, Z.; Mo, Z.; Liang, G.; Liu, H.; Huang, J.; Li, H.; Junchao, Y.; Mao, J.; Lin, K.; Mo, L. Pollution Characteristics and Source Apportionment of Organic Carbon and Elemental Carbon in PM 10 and PM 2.5 in Baise. Adm. Tech. Environ. Monit. 2019, 31 (2), 16–20. https://doi.org/10.3969/j.issn.1006-2009.2019.02.004. (in Chinese).
39. Zhang, L.; Ji, Y. Q.; Zhang, J.; Wang, S. B.; Li, Y. Y.; Zhao, J. Q.; Zhang, W. Characteristics and Sources of Carbon Components in PM 2.5 During Autumn and Winter in Panjin City. Environ. Sci. 2018, 39 (7), 3051–3056. https://doi.org/10.13227/j.hjkx.201712118. (in Chinese).

40. Zhang, J.; Han, L.; Cheng, S.; Wang, X.; Zhang, H. Characteristics and Sources of Carbon Pollution of Fine Particulate Matter in Typical Cities in Beijing-Tianjin-Hebei Region. Res. Environ. Sci. 2020, 33 (8), 1729–1739. https://doi.org/10.13198/j.issn.1001-6929.2020.02.12. (in Chinese).
41. Wang, G.; Kawamura, K.; Lee, S.; Ho, K.; Cao, J. Molecular, Seasonal, and Spatial Distributions of Organic Aerosols from Fourteen Chinese Cities. Environ. Sci. Technol. 2006, 40 (15), 4619–4625. https://doi.org/https://doi.org/10.1021/es060291x.
42. Chen, J.; Guo, J.; Ji, Y. Pollution Characteristics and Sources of Carbon Components in PM2.5 during Spring in Jinzhou City. Environ. Sci. Technol. 2020, 43 (10), 165–170. https://doi.org/10.19672/j.cnki.1003-6504.2020.10.022. (in Chinese).
43. Wang, C.; Yan, Y.; Duan, X.; Deng, M.; Wang, J.; Li, R.; Peng, L. Pollution Characteristics and Sources Analysis of Carbonaceous Aerosols in PM2.5 in Yangquan. Environ. Chem. 2021, 40 (5), 1442–1451. https://doi.org/10.7524/j.issn.0254-6108.2020102204. (in Chinese).
44. Yang, Y.; Tao, J.; Zhu, L.; Zhang, Z.; Wang, Q.; Cao, J. Characterization of Chemical Compositions of PM2.5 and Its Impact on Scattering Coefficients at a Background Site over Western China. Acta Sci. Circumstantiae 2017, 37 (4), 1216–1226. https://doi.org/Characterization of chemical compositions of PM2.5 and its impact on scattering coefficients at a background site over Western China. (in Chinese).
45. Qu, Y. et al. Spectral dependence of light absorption and direct radiative forcing of the TSP, PM10, PM2.5 and PM0.1 in a rural region of northwestern China. ATMOSPHERIC ENVIRONMENT **292**, (2023).
46. Liu, X. et al. Secondary Formation of Atmospheric Brown Carbon in China Haze: Implication for an Enhancing Role of Ammonia. ENVIRONMENTAL SCIENCE & TECHNOLOGY **57**, 11163–11172 (2023).
47. Sun, J. et al. Measurement report: Long-term changes in black carbon and aerosol optical properties from 2012 to 2020 in Beijing, China. ATMOSPHERIC CHEMISTRY AND PHYSICS **22**, 561–575 (2022).
48. Zhu, C.-S. et al. Black Carbon and Secondary Brown Carbon, the Dominant Light Absorption and Direct Radiative Forcing Contributors of the Atmospheric Aerosols Over the Tibetan Plateau. GEOPHYSICAL RESEARCH LETTERS **48**, (2021).
49. Wang, Q. et al. Exploring the variation of black and brown carbon during COVID-19 lockdown in megacity Wuhan and its surrounding cities, China. SCIENCE OF THE TOTAL ENVIRONMENT **791**, (2021).

50. Lin, Y.-C., Zhang, Y.-L., Xie, F., Fan, M.-Y. & Liu, X. Substantial decreases of light absorption, concentrations and relative contributions of fossil fuel to light-absorbing carbonaceous aerosols attributed to the COVID-19 lockdown in east China. ENVIRONMENTAL POLLUTION **275**, (2021).
51. Zhang, Q. et al. Investigation of Primary and Secondary Particulate Brown Carbon in Two Chinese Cities of Xi'an and Hong Kong in Wintertime. ENVIRONMENTAL SCIENCE & TECHNOLOGY **54**, 3803–3813 (2020).
52. Gao, Y. et al. Optical properties of mountain primary and secondary brown carbon aerosols in summertime. SCIENCE OF THE TOTAL ENVIRONMENT **806**, (2022).
53. Wang, Q. et al. High Contribution of Secondary Brown Carbon to Aerosol Light Absorption in the Southeastern Margin of Tibetan Plateau. GEOPHYSICAL RESEARCH LETTERS **46**, 4962–4970 (2019).
54. Zhang, Q. et al. Spatial distribution and sources of winter black carbon and brown carbon in six Chinese megacities. SCIENCE OF THE TOTAL ENVIRONMENT **762**, (2021).
55. Xu, B. et al. Light absorption properties and source contributions of black and brown carbon in Guangxi, southern China. ATMOSPHERIC RESEARCH **302**, (2024).
56. Guo, Z. et al. The optical properties and in-situ observational evidence for the formation of brown carbon in clouds. ATMOSPHERIC CHEMISTRY AND PHYSICS **22**, 4827–4839 (2022).
57. Wang, Q. et al. Optical source apportionment and radiative effect of light-absorbing carbonaceous aerosols in a tropical marine monsoon climate zone: the importance of ship emissions. ATMOSPHERIC CHEMISTRY AND PHYSICS **20**, 15537–15549 (2020).
58. Liu, X. et al. Emission characteristics and light absorption apportionment of carbonaceous aerosols: A tunnel test conducted in an urban with fully enclosed use of E10 petrol. ENVIRONMENTAL RESEARCH **216**, (2023).
59. Li, H. et al. Continuous Measurement and Molecular Compositions of Atmospheric Water-Soluble Brown Carbon in the Nearshore Marine Boundary Layer of Northern China: Secondary Formation and Influencing Factors. JOURNAL OF GEOPHYSICAL RESEARCH-ATMOSPHERES **128**, (2023).
60. Xie, F. et al. Decrease of atmospheric black carbon and CO2 concentrations due to COVID-19 lockdown at the Mt. Waliguan WMO/GAW baseline station in China. ENVIRONMENTAL RESEARCH **211**, (2022).

61. Cao, N. et al. Spatiotemporal distribution, light absorption characteristics, and source apportionments of black and brown carbon in China. SCIENCE OF THE TOTAL ENVIRONMENT **919**, (2024).